ELSEVIER

Catalysis Today 75 (2002) 95–102

CATALYSIS TODAY

www.elsevier.com/locate/cattod

Removal of cyanides in wastewater by supported TiO_2-based photocatalysts

J. Aguado, R. van Grieken*, M.J. López-Muñoz, J. Marugán

ESCET, Universidad Rey Juan Carlos, C/Tulipán s/n, 28933 Móstoles, Madrid, Spain

Abstract

Titania supported samples on different types of silica have been prepared through a sol–gel method followed by hydrothermal processing. The photocatalytic activity of the samples was tested for free cyanides photo-oxidation. As compared to commercial TiO_2 all the synthesised materials showed not only similar photocatalytic efficiencies but improved recovery properties. The degradation of iron(III) cyanocomplexes was also studied in the absence or presence of titania catalyst. In all cases, a photoinduced CN^- released from the complex takes place through a homogeneous process. The further oxidation of those cyanides ions to cyanate species is significantly enhanced in the presence of the catalyst in which mesostructured SBA-15 silica is used as support.

Keywords: Cyanide; Photocatalysts; Wastewater

1. Introduction

The presence of cyanides in effluents related to coal gasification and electroplating processes, in which metal cyanides utilisation is almost essential, is a matter of environmental concern not well resolved nowadays. Among the different technical alternatives to remove cyanides from industrial wastewater, photocatalytic processes have demonstrated a high efficiency [1]. Heterogeneous photocatalysis is based on the use of a source of UV radiation to stimulate a semiconductor material on whose surface the oxidation of the pollutant is carried out. In the last years, several environmental applications have been developed in this research field [2], titanium dioxide being the semiconductor most widely used due to its high activity. To maximise TiO_2 photoactivity, particles should be small enough to offer a high number of active centres by unit mass [3]. Unfortunately, a small particle size leads to high filtration costs to remove the catalyst, hindering its industrial application. For this reason, a major focus of current photocatalysis research is the achievement of titania-based materials with suitable properties to present simultaneously high photoactivity and effective separation properties. Titania nanoparticles supported on silica might be materials capable of accomplishing both requests since they do not only take the advantage of high surface areas but of improved recovery properties as compared to pure titania, which may facilitate the separation [4].

In the present work, the synthesis and characterisation of different TiO_2 supported on silica photocatalysts is reported as well as their application to the photo-oxidation of both free cyanides and complexed iron cyanides in water. The interest of testing the catalysts in the degradation of the latter species lies on the fact that none of the commercially available methods used up-to-date to treat wastewaters

* Corresponding author. Tel.: +34-91-488-7007; fax: +34-91-664-7490.
E-mail address: r.vangrieken@escet.urjc.es (R. van Grieken).

0920-5861/02/$ – see front matter
PII: S0920-5861(02)00049-4

polluted with cyanides are effective for the removal of iron cyanocomplexes species. Even though these compounds can be considered as nearly non-toxic themselves, in the presence of sunlight they are quite unstable dissociating the highly toxic free cyanide ions.

2. Experimental

2.1. Synthesis

The samples were prepared via sol–gel hydrolysis–condensation of titanium tetraisopropoxide in the presence of the chosen silica support: either a commercial SiO_2 (Crosfield CS 4187) or mesostructured MCM-41 and SBA-15 silica samples prepared in our laboratory. Textural properties of all the supports are summarised in Table 1. MCM-41 [5] was synthesised following a room temperature two-step sol–gel process based on a method recently reported [6]. In the first stage, a solution made up of hexadecyltrimethylammonium chloride ($C_{16}H_{33}(CH_3)_3NCl$, 25 wt.% aqueous solution, Aldrich) (CTMA) and hydrogen chloride (35 wt.% aqueous solution, Scharlab) with a molar ratio HCl:CTMA of 3.75 was prepared. Tetraethylorthosilicate ($Si(OC_2H_5)_4$, 99 wt.%, Alfa Chemicals) (TEOS) was added dropwise to the aqueous solution to give a molar ratio of CTMA:TEOS of 0.6 and the mixture was stirred at room temperature for 75 min. In the second step the condensation rate was increased by addition of a 2 wt.% aqueous ammonia solution until reaching a pH ∼ 4. After being aged for 1 h the solid was filtered, washed with deionised water, dried at 110 °C and calcined at 550 °C.

SBA-15 silica was prepared by dissolving Pluronic 123 (Aldrich) in 1.9 M HCl (weight ratio HCl:Pluronic of 31.25) at room temperature [7]. The solution was heated at 40 °C before the addition of TEOS (weight ratio Pluronic:TEOS of 2.18) and the mixture was vigorously stirred for 20 h at 40 °C. Following hydrothermal treatment at 110 °C for 24 h, the obtained solid was recovered by filtration, dried at room temperature and calcined at 550 °C.

To obtain the supported TiO_2/SiO_2 materials, a solution with the required amount of titanium tetraisopropoxide (TTIP) in isopropanol (*i*-PrOH) (weight ratio TTIP:*i*-PrOH of 1:8) was added to each support and the resulting mixture was stirred for 45 min at room temperature. Following deionised water addition (molar ratio H_2O:TTIP of 160), the stirring was maintained for 45 min and the solid was recovered by centrifugation, hydroprocessed at 110 °C and calcined at 550 °C. The nominal titania weight content of all the resulting supported materials was 20%. The codes used for naming those samples indicate in first place the type of silica support (Crosfield, MCM-41 or SBA-15) followed by "20% TiO_2".

2.2. Characterisation

The BET surface areas and pore volumes of the samples were determined from the N_2 adsorption–desorp-

Table 1
Textural properties (S_{BET}, V_P, D_P) and TiO_2 size (ϕ) of studied photocatalysts

Material	Specific surface area, S_{BET} ($m^2\,g^{-1}$)	Pore volume, V_P ($cm^3\,g^{-1}$)	Pore diameter, $D_{P(BJH-ADS)}$[a] (nm)	Particle diameter	
				$\phi_{XRD(Anat.)}$[b] (nm)	$\phi_{UV-VIS(Anat.)}$[c] (nm)
Degussa P-25 TiO_2	51.4	–	–	31 (54[d])	–
Acros anatase	7.2	–	–	129	–
Crosfield CS 4187 silica	265	1.53	23.0	–	–
MCM-41 silica	1051	0.83	1.9	–	–
SBA-15 silica	640	0.96	6.3	–	–
Crosfield/20% TiO_2	233	1.16	19.9	7.0	8.9
MCM-41/20% TiO_2	294	0.53	8.2	8.2	8.9
SBA-15/20% TiO_2	358	0.70	8.0	6.6	6.6

[a] Determined by BJH model.
[b] Determined by XRD broadening.
[c] Determined by UV–VIS.
[d] Rutile particle size.

tion at 77 K using a Micromeritics Tristar 3000 equipment. For the determination of the pore size distributions, the BJH model was applied assuming a cylindrical geometry of the pores.

Powder X-ray diffraction (XRD) patterns were acquired on a Philips X'PERT MPD diffractometer using monochromatic Cu Kα radiation and scanning 2θ from 20 to 70°. Calcite(1 0 4) peak ($2\theta \sim 29.4°$) was used as internal standard to calculate instrumental width.

Diffuse reflectance spectra in the 200–500 nm range were recorded with a Varian Cary 500 Scan UV–VIS–NIR spectrophotometer equipped with an integrating sphere diffuse reflectance accessory, using polytetrafluoroethylene as reference scatterer. The reflectance data were reported as $F(R_\infty)$ value which was obtained by application of the Kubelka–Munk algorithm. The band gap determination of the prepared samples was performed by plotting $[F(R_\infty)h\nu]^2$ versus $h\nu$ (eV) and calculating the x-axis intercept of the extrapolated linear section of the spectra. Settling curves of the different materials were also carried out in the UV–VIS spectrophotometer using the standard liquid cell holder, following the experimental procedure described below.

Transmission electron microscopy (TEM) images were taken on a JEOL JEM-2000 FX microscope working at 200 kV. Previously, the samples were dispersed in acetone, stirred in an ultrasonic bath and finally placed on a carbon-coated copper grid. Scanning electron microscopy (SEM) micrographs were taken on a JEOL JSM-6400 working at 20 kV and equipped with EDS analysis.

Chemical analysis for determining iron content of the catalysts after reaction were performed using a Varian VISTA AX inductive coupling plasma (ICP) equipment.

2.3. Photocatalytic reactions

The photocatalytic runs were carried out in a Pyrex batch reactor of cylindrical shape containing 1 l of the aqueous dispersion of the catalyst and the pollutant. The reactor was provided on the top with three ports for inflow and outflow of gases and withdrawal of aliquots for their analysis. All the irradiation runs were performed with a 150 W medium pressure mercury lamp (Heraeus TQ-150) inside a quartz jacket, coaxial with the photoreactor within the reaction mixture. The lamp was surrounded with a cooling tube in which an aqueous solution of copper sulphate was circulating to both prevent overheating of the suspension and cut off radiation with a wavelength shorter than 300 nm. For comparison of the photocatalytic activity of the prepared samples, in all experiments the amount of catalyst was adjusted to achieve a concentration of $0.5\,g\,l^{-1}$ in TiO_2. The removal of CN^- was followed either potentiometrically with a selective CN^- electrode (Orion 720A) or spectrophotometrically using a pyridine–barbituric acid reagent [8], depending on the cyanide concentration. Identification and quantification of the products were performed by ionic chromatography using a Metrohm apparatus (Separation centre 733, IC detector 732, Pump Unit 752) with reference standards. Aqueous solutions of $NaHCO_3$ (2 mM), and Na_2CO_3 (1.3 mM) were used as eluent. Prior to every photocatalytic run, the reaction mixture consisting of an aqueous solution containing 100 ppm of CN^- equivalents and the catalyst was bubbled with air for at least 15 min to ensure the presence of enough oxygen concentration at the beginning of the reaction. Simultaneously the lamp was switched on during those 15 min before immersing it in the reactor, to avoid the inherent induction time of the irradiation source. The reaction mixture was magnetically stirred during the run. Aliquots of 7 ml were taken at selected reaction times following filtration through 0.22 μm Nylon membranes before being analysed. Potassium cyanide and potassium hexacyanoferrate(III) (Scharlab, reagent grade) were used for the preparation of the cyanide solutions, and NaOH (Scharlab, reagent grade) for adjusting the initial pH of the reaction mixture.

2.4. Settling recovery tests

The separation of the catalyst particles after photoreaction is an important factor to make feasible this process in wastewater treatment. To measure such property in the different catalytic systems, a parameter was determined based on comparative gravitational settling of catalyst particles in water as described below. The studied sample was dispersed in deionised water under constant stirring for 15 min. The amount of catalyst in all experiments was adjusted to get a TiO_2 concentration of $0.5\,g\,l^{-1}$. Once a homoge-

neous suspension had been achieved, an aliquot was transferred to the UV–VIS spectrophotometer cell for liquids. Deposition of the suspended particles was monitored by means of the increasing of transmittance values measured at a wavelength of 550 nm versus time. For comparison of the settling recovery properties of the different samples we will refer to a "settling parameter", defined as the percentage of transmittance increase at $\lambda = 550$ nm, obtained after the first 5 min of sedimentation.

Two commercial samples were employed in the present study as references for both the settling recovery properties and the activity of the catalysts. These samples were supplied by Degussa (P25; anatase:rutile ratio of 4:1) and Acros (99% anatase).

3. Results and discussion

3.1. Catalysts characterisation

Textural properties of the photocatalysts are presented in Table 1. XRD patterns showed that anatase was the only crystalline phase present in all TiO_2 supported samples. Average diameter sizes of the titania particles were calculated from the broadening of the 1 0 1 XRD anatase peak. The obtained values were consistent with those obtained by analysis of the TEM micrographs and the calculated ones from the optical band gap applying the hyperbolic band model [9]. The morphology of the catalysts was examined by SEM. Fig. 1 shows the SEM micrographs of two selected samples, the commercial Degussa P25 and supported Crosfield/20% TiO_2. Whereas the latter sample is constituted by well-defined micro-size particles of silica with titania incorporated within the porous structure, commercial TiO_2 from Degussa consists of agglomerates of particles in the nanometer size, very difficult to separate from the aqueous solution. The morphology of the materials prepared with mesostructured silica, presents features halfway between both extremes. Most significantly, there is a homogeneous titania distribution in all the synthesised samples whatever the silica support, according to the chemical composition of the sample determined by energy dispersive analysis, which agrees with the nominal bulk composition.

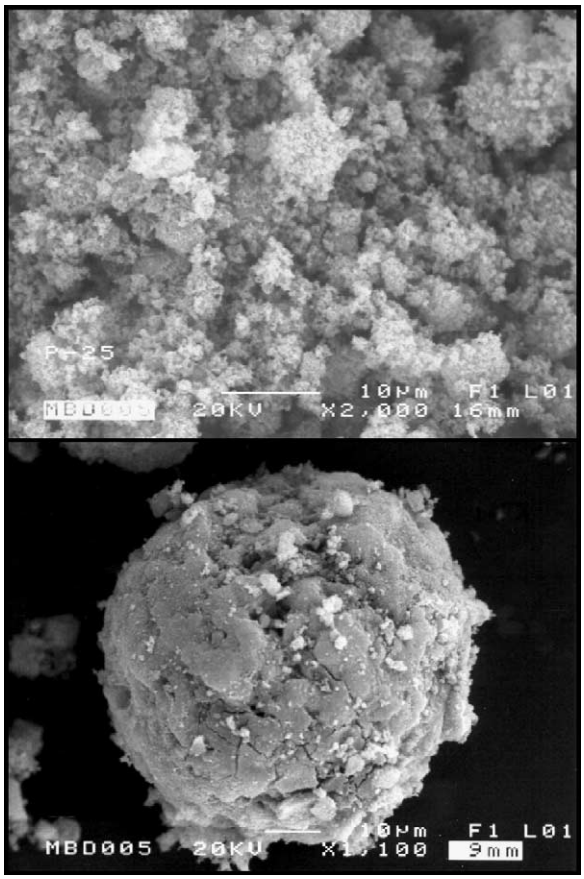

Fig. 1. SEM micrographs of Degussa P-25 and Crosfield/20% TiO_2 samples.

3.2. Reaction results

The activity of the titania samples for photo-oxidation of free cyanides was examined in first place. As it has been indicated, the quantity of sample used in each run was adjusted to achieve equal TiO_2 concentration ($0.5\,g\,l^{-1}$) for the purposes of comparing the activity of the different catalysts. The initial pH of the reacting solutions was 11.5. The amount of cyanide ions decreased with increasing irradiation time in the presence of each and every catalyst. No cyanide oxidation was found in the absence of either catalyst, source of light or air thus indicating the photocatalytic nature of the studied processes. Fig. 2 shows the percentage of cyanide photo-oxidation accomplished with each sample after 4 h of reaction together

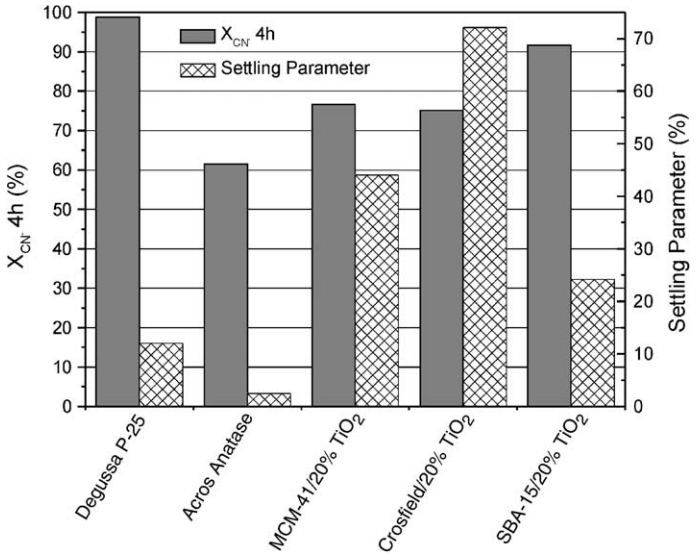

Fig. 2. Results of CN^- photo-oxidation and settling recovery of studied photocatalysts.

with the corresponding "settling recovery parameter" calculated by following the procedure described in Section 2. The analysis by ionic chromatography of the species along the reaction showed the formation of cyanate as the first photo-oxidation product. Once the complete cyanide disappearance had been achieved nitrate species were detected thus indicating they are produced by the subsequent CNO^- oxidation. The results are in agreement with the mechanism previously proposed by Augugliaro et al. [1]. Since the commercial TiO_2 samples used in this work (Degussa P25 and Acros anatase) have only external surface, differences found in their reactivity might be explained according to their respective BET surface areas. As compared with the commercial samples, it is observed that all the synthesised TiO_2/SiO_2 samples achieved conversions for cyanide photodegradation higher than Acros anatase. It is remarkable the SBA-15/20% TiO_2 sample whose activity is close to that obtained with Degussa P25. The latter, is the most widely studied titania catalyst due to its high activity, so its activity is taken as point of reference in many photocatalytic processes. However, the recovery of the catalyst by filtration once the reaction has been finished is a problem not solved at the moment. For this reason, it is noticeable the important improvement of the settling recovery properties shown for the synthesised samples as compared to both titania Degussa P25 and Acros commercial samples.

On the basis of the results obtained for free cyanides, further investigations were performed on the photodegradation of hexacyanoferrate(III) ions with the samples which had shown higher activity, that is, Degussa P25 and SBA-15/20% TiO_2. The mechanism and kinetics of degradation under UV radiation of complexed cyanides have been previously studied [10,11]. It has been reported that iron(III) cyanocomplexes are degraded through a homogeneous photochemical mechanism under UV and/or near UV radiation. Therefore, preliminary experiments were carried out irradiating hexacyanoferrate(III) solutions without addition of catalyst. Fig. 3 shows the comparison of the results obtained without added catalyst and with both selected titania Degussa P25 and the SBA-15/20% TiO_2 catalysts. All the reaction runs were performed at initial pH 11 and hexacyanoferrate(III) concentration 0.64 mM. As our main objective was to study the release and fate of cyanide ions in the process, both the concentration of $[Fe(CN)_6]^{3-}$ and cyanate ions are expressed as ppm of $[CN^-]$ (i.e. 0.64 mM $[Fe(CN)_6]^{3-}$ corresponds to 100 ppm of $[CN^-]$ and 161.5 ppm of $[CNO^-]$ are equivalent to 100 ppm of $[CN^-]$). On the basis that free CN^- and CNO^- were the only species detected

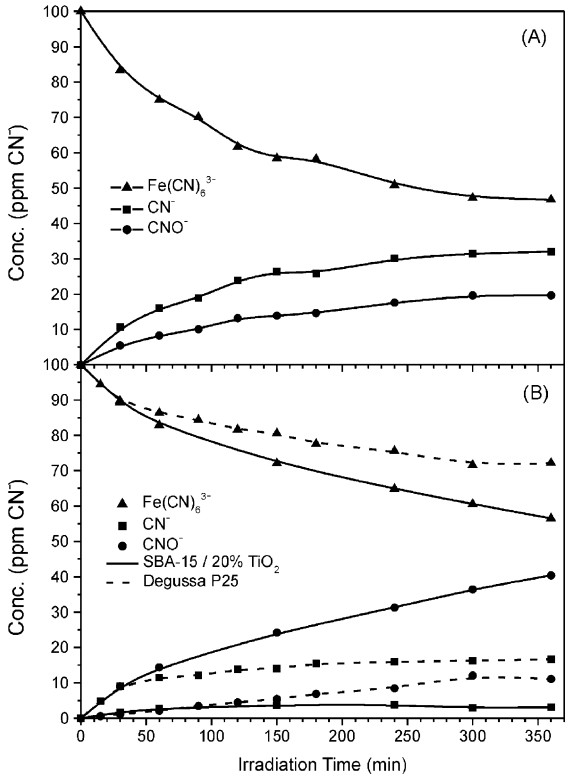

Fig. 3. Concentrations of complexed cyanide, cyanide and cyanate species vs. irradiation time in the (A) absence and (B) presence of SBA-15/20% TiO_2 and Degussa P25 catalysts.

during the photoreactivity runs shown in Fig. 3, complexed cyanide concentration at increasing irradiation times was calculated as the difference between the initial $[Fe(CN)_6]^{3-}$ concentration and the sum of free cyanide and cyanate concentrations. In the absence of catalyst, it was detected the release from the complex of cyanide ions and the formation of cyanate species thus confirming the existence of a homogeneous degradation. Whereas the former experimental feature may be explained by means of a photoinduced substitution of the cyanide ligands in the complex by hydroxyl groups and/or water molecules [10,11], the origin of cyanate formation in such case is not clear taking into account we are just using a medium pressure Hg lamp as source of UV radiation. A plausible explanation which has been previously suggested [10] is the assumption that the various soluble iron(III)-containing species formed during the irradiation are responsible for the oxidation of released CN^- to CNO^-. Those iron(III) species yielded the formation of $Fe(OH)_3$, as a reddish brown precipitate was formed during the reaction [12]. The results obtained in the presence of TiO_2 Degussa P25 or SBA-15/20% TiO_2 showed that their respective activities for the removal of complexed cyanides were lower than the ones obtained for the photo-oxidation of free cyanides at equal irradiation times. Moreover, as compared with the homogeneous system the commercial catalyst markedly decreases the final achieved decomposition of the cyanocomplexes. It has been suggested [11] that the cyanocomplexes photo-oxidation in the presence of catalyst, oxygen and high energy UV radiation proceeds by two simultaneous mechanisms: a homogeneous process through which free cyanide ions are released from the complex and a heterogeneous route in which the catalyst promotes the subsequent oxidation of released cyanide to cyanate species [11]. Assuming such mechanism in our system, the observed detrimental effect of the titania particles for the cyanocomplexes degradation may be ascribed to a reduced efficiency of the reacting solution in the photon absorption that leads to the release of free cyanides. The competition for the photons between the titania particles and the hexacyanoferrate(III) species results in a lower activity of the overall degradation process if compared to the absence of solid particles in the reaction medium. Such screening effect of the titania particles is greatly reduced if they are fixed on a transparent support to the used UV radiation, as it is indicated by the percentage of cyanocomplexes degradation obtained in the presence of the SBA-15/20% TiO_2 catalyst, which is very similar to the one achieved in the homogeneous system. Most significant, is the difference in the cyanide and cyanate concentrations found along the reaction in both the systems. According to the experimental results, the homogeneous mechanism is quite efficient for the breaking of cyanide bonds in the complex but not so much for their further oxidation. The danger of exposure of hexacyanoferrate(III) solutions to solar radiation lies on this fact, due to the release of highly toxic free cyanides. By contrast, in the presence of the SBA-15/20% TiO_2 catalyst the free cyanide concentration remains at low levels during the irradiation (Fig. 3) since an effective cyanate production takes place through the heterogeneous photocatalytic route.

Longer irradiation times than those presented in Fig. 3 resulted in further nitrates formation.

Once the irradiation experiment had been concluded the catalysts were recovered by filtration. A substantial difference between both catalyst samples was observed; whereas Degussa P25 TiO_2 presented the reddish brown colour indicative of the presence of $Fe(OH)_3$, the SBA-15/20% TiO_2 catalyst appeared completely white. The ICP analysis of the recovered catalysts revealed the presence of iron in the latter sample. We have not elucidated at the moment the nature of the iron-containing species remaining on the SBA-15/20% TiO_2 catalyst, but iron(III) hydroxide can be discarded on the basis of the white colour. As the activity for free cyanides photo-oxidation found for Degussa P25 is higher than for SBA-15/20% TiO_2 (Fig. 2), once CN^- ions are released from the complex we would expect a higher photocatalytic oxidation activity and thus a higher cyanate production for the former catalyst as compared to the latter. According to Augugliaro et al. [11] the occurrence of $Fe(OH)_3$ formation varies the irradiation conditions of the system due to the shielding effects produced by the presence of the hydroxide flocs. The shielding effect of the $Fe(OH)_3$ species formed in the presence of Degussa P25 may contribute to the decrease in activity of the heterogeneous route with this catalyst. On this basis, it might be explained the different CN^-:CNO^- ratio found in each heterogeneous system during the hexacyanoferrate(III) degradation process. Moreover, the metal adsorption on the TiO_2 surface may also have a detrimental effect on the activity [10] as it can block or inactivate centres of the photocatalyst. However, if iron adsorption would take place preferentially on the silica, more active centres would be available on the titania particles preventing the decrease in the global reaction observed when just TiO_2 is used as catalyst. This would remark the beneficial effect of the SiO_2 support, which shows no photoactivity but may offer proper adsorption sites for the iron species resulting from the breakage of the complex.

4. Conclusions

Titania supported over a porous silica, a host that is transparent to the employed UV radiation, is shown to be a good method for developing TiO_2-based materials with reasonable activity for cyanide photocatalytic oxidation and improved separation properties. The type of the silica host affects not only the TiO_2 size or the recovery properties of the catalysts but also, the activity of each sample. The use of mesostructured silica SBA-15 leads to the best activity of the supported titania, comparable to that obtained with Degussa P25 in the removal of free cyanides but showing improved settling properties.

In the absence of catalyst a homogeneous degradation of iron(III) cyanocomplexes is observed, producing the release of cyanide ions from the complex and some further oxidation to CNO^- species. In the presence of the titania catalysts besides the homogeneous process, a heterogeneous mechanism in which the catalyst promotes the subsequent oxidation of released cyanide to cyanate species takes place. The best performance to achieve the oxidation of iron(III) cyanocomplexes to cyanate species is obtained with the SBA-15/20% TiO_2 catalyst. The higher efficiency of this material as compared with Degussa P25 can be attributed to the following: (i) it minimises the screening effect of bare titania particles in the homogeneous process; (ii) it prevents the formation of $Fe(OH)_3$ flocs and their shielding effect on titania particles; (iii) the silica support may offer proper adsorption sites for the iron species resulting from the breakage and reaction of the complex.

Acknowledgements

The authors thank “Consejería de Educación, Comunidad de Madrid” for the financial support of this research through the project 07M/0050/1998 and “Grupos Estratégicos de Investigación” and “CICYT” through the project PPQ2000-1287.

References

[1] V. Augugliaro, V. Loddo, G. Marcì, L. Palmisano, M.J. López-Muñoz, J. Catal. 166 (1997) 272.
[2] M. Anpo, Stud. Surf. Sci. Catal. 130 (2000) 157.
[3] Z. Zhang, C.C. Wang, R. Zakaria, J.Y. Ying, J. Phys. Chem. B 102 (1998) 10871.
[4] B.J. Aronson, C.F. Blanford, A. Steïn, Chem. Mater. 9 (1997) 2842.
[5] C.T. Kresge, M.E. Leonowicz, W.J. Roth, J.C. Vartuli, J.S. Beck, Nature 359 (1992) 710.
[6] J. Aguado, D.P. Serrano, J.M. Escola, Micropor. Mesopor. Mater. 34 (2000) 43.

[7] D. Zhao, J. Eng, Q. Huo, N. Melosh, G.H. Fredrickson, B.F. Chmelka, G.D. Stucky, Science 279 (1998) 548.
[8] L.S. Clesceri, A.E. Greenberg, A.D. Eaton (Eds.), Standard Methods for the Examination of Water and Wastewater, 20th Edition, American Public Health Association, 1998.
[9] Y. Wang, A. Suna, W. Mahler, R. Kasowski, J. Chem. Phys. 87 (1987) 7315.
[10] W. Scott Rader, L. Solujic, E.B. Milosavljevic, J.L. Hendrix, Environ. Sci. Technol. 27 (1993) 1875.
[11] V. Augugliaro, E. García-López, V. Loddo, G. Marcì, L. Palmisano, Adv. Environ. Res. 3 (2) (1999) 179.
[12] D.R. Lide (Ed.), Handbook of Chemistry and Physics, CRC Press, Boca Raton, FL, USA, 1996.